Quiet time variability of the GPS TEC and EEJ strength over Indian region associated with major sudden stratospheric warming events during 2005/2006

S. Sripathi[1] and A. Bhattacharyya[1]

Received 24 August 2011; revised 2 March 2012; accepted 19 March 2012; published 3 May 2012.

[1] This paper describes the quiet time variabilities of the ionospheric total electron content (TEC) derived from the signals from Global Positioning Satellite System (GPS) recorded at several stations in India along with simultaneous observations of equatorial electrojet (EEJ) strength obtained from geomagnetic field variations during January–March 2006 when sudden stratospheric warming (SSW) events occurred. Analysis of the observations presented here confirms that strong correlation exists among the variabilities in EEJ strength and GPS TEC observations. Investigations suggest that there exist large-scale wave like structures with periodicity of quasi 16-day wave in the TEC observations near the equatorial ionization anomaly (EIA) crest quite similar to that of EEJ strength. Our observations also indicate the existence of morning enhancement and evening reduction of TEC and EEJ strength and vice versa during SSW events similar to that reported elsewhere. Using these observations, it is suggested that the quiet time variabilities seen in the GPS TEC over EIA could be caused due to the nonlinear interaction of upward propagating planetary waves (PWs) with atmospheric tides. Presence of similar periods in the EEJ strength and TEC observations near the EIA crest region, supports the view that the large-scale wave like structures seen in TEC near the EIA crest are associated with PWs that are modifying the primary eastward electric field in the equatorial E region and hence the EEJ strength through non linear interactions with atmospheric tides.

Citation: Sripathi, S., and A. Bhattacharyya (2012), Quiet time variability of the GPS TEC and EEJ strength over Indian region associated with major sudden stratospheric warming events during 2005/2006, *J. Geophys. Res.*, *117*, A05305, doi:10.1029/2011JA017103.

1. Introduction

[2] The seasonal and latitudinal variations in the different regions of the ionosphere during magnetically quiet and disturbed conditions have been studied extensively over several years using both observations and theory [e.g., *Rastogi and Sharma*, 1971; *Gupta and Singh*, 2000; *Fejer et al.*, 1991; *Fuller-Rowell et al.*, 1997; *Araujo-Pradere et al.*, 2005]. However, the day-to-day variabilities in the different regions of the ionosphere are not yet fully understood [e.g., *Dabas et al.*, 1984; *Alex and Rastogi*, 1989; *Forbes et al.*, 2000; *Rishbeth and Mendillo*, 2001; *Pancheva et al.*, 2002, 2008]. Since the day-to-day variabilities play a vital role in understanding several physical processes, it is essential to understand these variations quantitatively. *Forbes et al.* [2000] have studied the variability of maximum electron density of the F_2 layer (N_mF_2) quantitatively using foF_2 data obtained from nearly 100 ionosonde stations. Their study indicates that the day-to-day variabilities under quiet time conditions could account for ∼25–35% at higher frequencies and ∼15–20% at low frequencies at all latitudes. TIME-GCM/CCM3 model results suggested that while the day-to-day variability is found to be better correlated with the variations in the winds than with the variations in the thermospheric neutral composition, annual and semiannual variations of the F_2 layer is mainly caused by the neutral composition [*Mendillo et al.*, 2002]. As the Earth's ionosphere is located at a transition region where it has the influence of solar wind dynamic pressure from the top and influence of the lower atmospheric waves originating from the bottom, understanding and modeling the day-to-day variabilities are highly complicated [e.g., *Rishbeth and Mendillo*, 2001].

[3] The observational database suggests that the day-to-day variabilities in the ionosphere could be caused by mostly (a) atmosphere–ionosphere coupling, (b) solar flux and (c) geomagnetic storms [e.g., *Forbes et al.*, 2000]. While geomagnetic storms do affect the ionosphere over equatorial and low latitudes, their influences are predominantly seen over high latitudes [e.g., *Forbes et al.*, 2000]. On the other

[1]Indian Institute of Geomagnetism, Navi Mumbai, India.

Corresponding Author: S. Sripathi, Indian Institute of Geomagnetism, Navi Mumbai 410216, India. (sripathi@iigs.iigm.res.in)

0148-0227/12/2011JA017103

hand, vertical coupling due to neutral atmospheric waves such as gravity waves, tides or planetary waves (PWs) is an important source for the variabilities in the equatorial and low latitude ionosphere. It may be pointed out here that gravity waves have periods of a few 10s of minutes and tides have periodicities in the sub-harmonics of 24 h but the PWs have periods ranging from 2 days to 2 weeks [*Madden*, 1979]. The PWs are usually global scale oscillations identified as the manifestation of the resonant or Rossby normal mode oscillations of the atmosphere [*Salby*, 1984]. The horizontal and vertical scales of the normal modes are strongly affected by the background neutral wind and temperature structure through which they propagate. As they propagate to the higher altitudes, due to exponential decrease of atmospheric density, the amplitude of the wave keeps increasing. Most of these atmospheric waves propagate to the mesosphere lower thermosphere (MLT) region and start to break and dissipate their energy. The PWs may thus interact with or modulate the diurnal/semi-diurnal tides and gravity waves over MLT region and may lead to changes in the ionospheric vertical drift or vertical transport through dynamo effect, which could act as a source for the ionospheric variability.

[4] The equatorial electrojet (EEJ) electric fields are generated by atmospheric tides through dynamo action wherein a conducting fluid moves across the geomagnetic field; and any modulation of *E* region winds by planetary waves would produce oscillations of the equatorial electric field [*Forbes and Leveroni*, 1992]. The effect of this oscillation would in turn show up in the distribution of plasma in the EIA region. The EEJ strength derived from measurements of the horizontal component H of the geomagnetic field at a location close to the dip equator and another away from the influence of the EEJ has been shown to be linearly related to the daytime, vertical drift of the plasma in the equatorial *F* region [*Anderson et al.*, 2002]. The equatorial *F* region plasma rises until pressure gradients are high enough for the plasma to move down along the geomagnetic field lines, assisted by gravity, toward the tropical latitudes away from the dip equator to form the EIA through the well known fountain effect which was first suggested by *Rastogi* [1959]. Hence there exists a close relationship between peak strength of the EEJ and strength of the EIA [*Sethia et al.*, 1980; *Balan and Iyer*, 1983; *Rastogi and Klobuchar*, 1990; *Bagiya et al.*, 2009]. Recently, *Liu et al.* [2010] have modeled the ionospheric variability during solar minimum conditions when PWs are excited in the winter stratosphere using TIME-GCM model. The model results suggest that PW and tidal interaction leads to large changes in the tides, which can strongly impact the ionosphere at low and midlatitudes through E region wind dynamo. *Fagundes et al.* [2009a, 2009b] found a post-sunset height rise of the F layer due to greater pre-reversal enhancement (PRE), which was attributed to traveling PWs. Further, they showed that day-to-day variability of the equatorial spread F (ESF) is closely related to the PRE modulation due to PWs. Hence, it is important to understand the day-to-day variabilities of the equatorial and low latitude ionosphere under quiet time conditions which cause the variabilities of ESF and radio wave scintillations.

[5] While some studies have been made to understand the day-to-day variabilities of the ionosphere due to vertical coupling from MLT region [e.g., *Parish et al.*, 1994; *Forbes and Leveroni*, 1992], recently many studies have focused on understanding the role of vertical coupling in the day-to-day variability of the ionosphere due to Sudden Stratospheric Warming (SSWs) events [e.g., *Liu and Roble*, 2002, 2005; *Hoffmann et al.*, 2007; *Chau et al.*, 2009, 2010; *Sridharan et al.*, 2009; *Goncharenko et al.*, 2010a, 2010b; *Fejer et al.*, 2010; *Yue et al.*, 2010; *Pedatella and Forbes*, 2010]. These studies revealed that while SSW events are indeed found to affect the ionosphere significantly, the physical processes responsible for generating such variability are not yet fully established. For example, the anomalous increase in the vertical drift velocity over Jicamarca Radio Observatory (JRO) during SSW events is suggested to be due to an anomalous increase of PWs [e.g., *Chau et al.*, 2009]. Based on TEC observations and modeling results, *Goncharenko et al.* [2010a] have suggested that there is a strong association between the perturbations in the high-latitude stratosphere and the variation noticed in low-latitude ionosphere. Interestingly, their study showed semidiurnal wave signature which is producing major ionospheric variations. Using GCM model, they interpreted their observations in terms of large-scale changes in atmospheric tides due to nonlinear interaction with planetary waves during SSW events. Further, *Goncharenko et al.* [2010b] have suggested that the phase of the semi-diurnal perturbations progressively shifts to later local times in subsequent days and the shift is different for different SSW events. In addition, some of the recent studies have also explored such connections in mesospheric wind, counter electrojet (CEJ) and TEC observations during SSW events [e.g., *Vineeth et al.*, 2007, 2009; *Sridharan et al.*, 2009; *Sathishkumar and Sridharan*, 2009; *Pedatella and Forbes*, 2010]. The anomalous increase in temperature and decrease of zonal mean winds at stratospheric altitudes in high latitudes have been found to be associated with anomalous decrease in temperature and increase in zonal mean wind over low midlatitudes at stratospheric altitudes [*Mukhtarov et al.*, 2007]. According to some studies, this pattern may extend to the mesosphere and lower thermosphere [*Shepherd et al.*, 2007; *Pancheva et al.*, 2008]. The key mechanism for the vertical coupling during SSW events is believed to be the nonlinear interaction of PWs and migrating tides [*Sridharan et al.*, 2009; *Liu et al.*, 2010; *Pedatella and Forbes*, 2010]. *Fuller-Rowell et al.* [2010] have observed the effects of SSW events using Whole Atmosphere Model (WAM) and suggested that it is possible that major SSWs could cause large changes in the thermospheric dynamics and electrodynamics that result in TEC variations. At low latitudes, day-to-day variability of the EIA can be attributed to the day-to-day changes in the ionospheric dynamo in the equatorial region, which is produced by atmospheric tides. Thus modulations in the tidal wind field during SSW events would produce modulations in the zonal electric field at the dip equator and hence influence the EIA as studied by *Pedatella and Forbes* [2010] using global ionosphere maps derived from GPS observations from the International GNSS (Global Navigation Satellite System) Service (IGS).

[6] In this paper, we study the variations in the equatorial and low latitude ionosphere in the Indian region during major SSW events that occurred during the northern winter period of 2005/2006. For this, we have used total electron

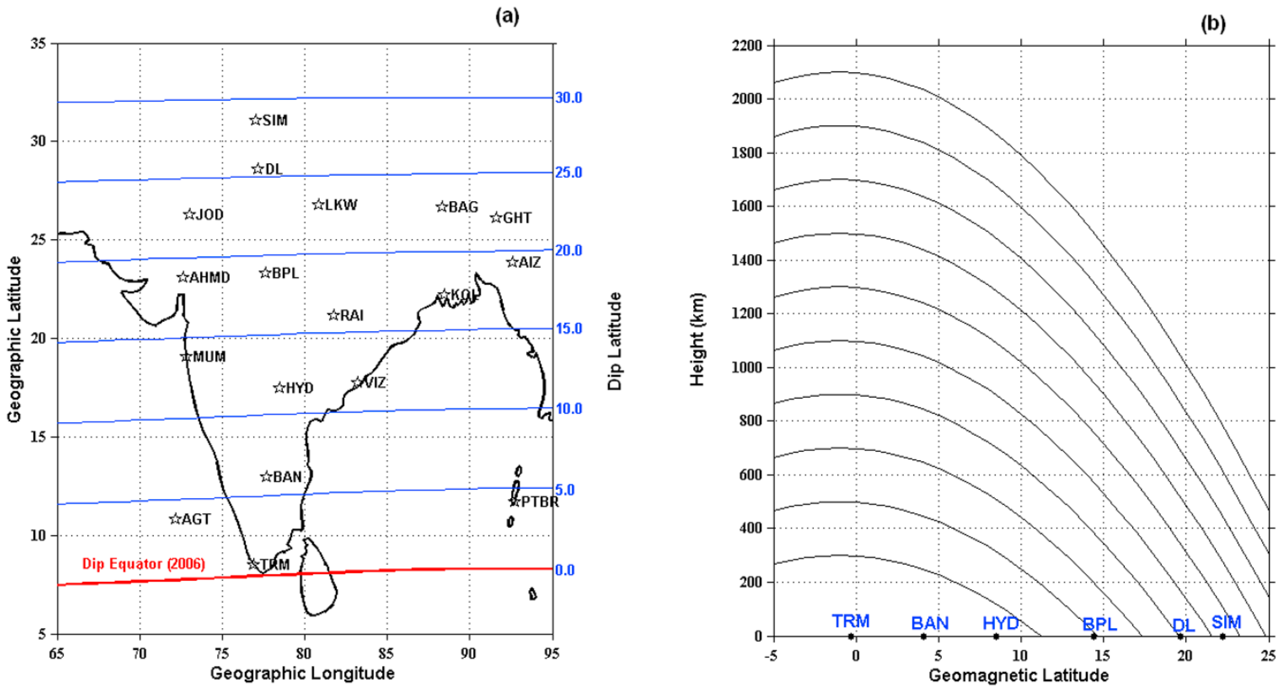

Figure 1. The (a) locations and (b) their altitude-latitude connection of dual frequency GPS receiver stations installed in the Indian sector under GAGAN project.

content (TEC) data from observations carried out with a network of dual frequency GPS receivers in India along with horizontal geomagnetic field data from an equatorial and an off-equatorial station in India, during January to March 2006. It should be pointed out that during the period under consideration there were only two IGS stations in India. While several studies indicate the existence of day-to-day variabilities in the ionosphere over Indian region [*Rastogi et al.*, 1973; *Rama Rao et al.*, 2006; *Bagiya et al.*, 2009], due to lack of continuous observations, the impact of PWs during major SSW events on the ionospheric TEC has not been studied in detail. Now simultaneous measurements of GPS TEC using a chain of GPS receivers along with continuous observations of ground magnetometers obtained at Tirunelvali and Alibag stations provides an excellent opportunity to study the ionospheric variabilities associated with SSW events.

2. Experimental Details

[7] The observations reported here were made using 18 dual frequency GPS receivers installed under the GPS aided geo-augmented navigation (GAGAN) project [e.g., *Sripathi et al.*, 2011]. Figure 1a shows the geographic location of GPS receiver stations, while Figure 1b shows the configuration of geomagnetic field lines assumed to be due to a tilted centered dipole for different apex heights of the field lines above the geomagnetic equator. The apex heights cover a range extending from 300 km to 2100 km in steps of 200 km. Figure 1b can be used to picture how high the ionospheric plasma has to reach above the geomagnetic equator in order to diffuse down to say 300 km altitude above an off-equatorial station. Geomagnetic latitude of the 6 GPS stations within the 75–80°E geographic longitude band are indicated on Figure 1b. Each GPS receiver can track up to 11 satellites at a given time. The data collected for every 1 min interval provides statistical parameters like S_4 index (which is the standard deviation of normalized intensity of the signal), the standard deviation of phase and the receiver lock time for each satellite being tracked. The GPS satellites transmit radio signals at two frequencies namely L1 (1575.75 MHz) and L2 (1227.25 MHz). The dispersive nature of the ionosphere causes these two radio signals to propagate at different velocities, producing a time delay. This time delay is proportional to the TEC along the line of sight to the satellite. Using the time delays from these two radio signals and also the more accurate phase information, the slant TEC (STEC) is obtained. From the STEC, the vertical TEC (VTEC) is calculated using appropriate mapping function, $S_f = \cos\chi$, i.e., VTEC = STEC* $\cos\chi$ where $\chi = \sin^{-1}[R_E \cos\alpha/(R_E + h)]$, α is the elevation angle, R_E = Earth's radius, h = 400 km. The VTEC (henceforth called as TEC) data used in the present study was computed from ground based GPS measurements by the application of a Kalman filter technique to eliminate the receiver and satellite instrument biases.

[8] The 1 min ground data for the horizontal component H of the geomagnetic field from Tirunelveli (8.7°N, 77.8°E, dip latitude: 0.4°N) and Alibag (18.5°N, 72.9°E, dip latitude: 13.0°N) are used to obtain the variation (ΔH) in H from the midnight baseline for each station to eliminate the contribution of earth's main field from the data. The strength of the equatorial electrojet is given by $\Delta H = (\Delta H)_{Tirunelveli} - (\Delta H)_{Alibag}$ [*Rastogi and Klobuchar*, 1990]. In addition, the zonal wind and temperature observations at polar stratospheric altitudes obtained from the National Centers for Environmental Prediction (NCEP), the solar flux at F10.7 cm

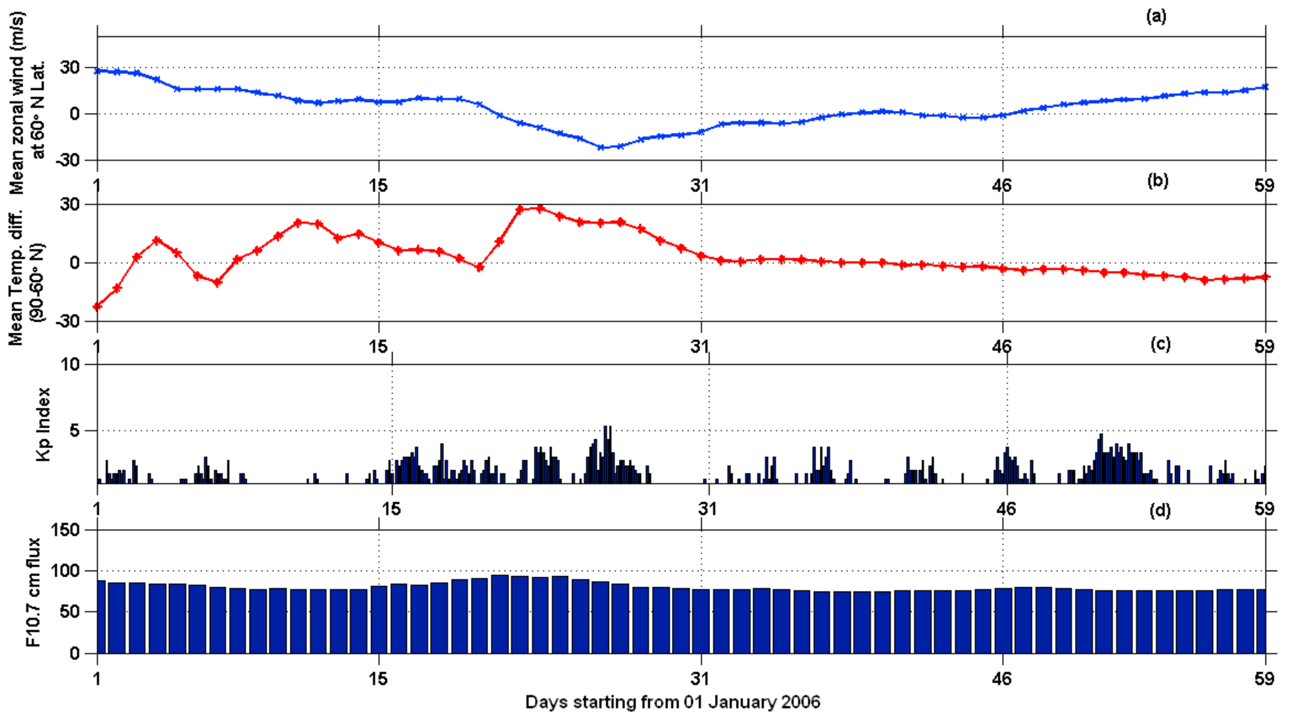

Figure 2. The NCEP (a) mean zonal winds at 60°N, (b) temperature difference between 90°N and 60°N respectively at polar stratospheric altitudes (at 10 hPa), (c) 3 hourly Kp Index, and (d) F10.7 cm flux as a function of day number during 1 January 2006–28 February 2006.

and 3 hourly Kp index for the corresponding period, are also used in the present study.

3. Results

3.1. NCEP Mean Zonal Wind and Temperature Over Polar Region

[9] Figures 2a–2d show the NCEP mean zonal winds at 60°N latitude (Figure 2a), zonally averaged temperature difference between 90°N and 60°N at polar stratospheric altitudes (at 10 hPa) respectively (Figure 2b), 3-hourly Kp index (Figure 2c), and solar flux at F10.7 cm (Figure 2d) as a function of day number during 1 January 2006–28 February 2006. The wind observations shown in Figure 2a reveal that the mean zonal wind initially positive and about 25 m/s, gradually decreases and goes below zero between days 20–30; it slowly increases thereafter and becomes positive again. On the other hand, mean temperature difference shown in Figure 2b reveals that it is negative in the initial period but later on it changes to positive and becomes 10 K on day number 4 which is considered to be weak SSW event. After that it suddenly decreases to -10 K on day number 7 and again it goes to 20 K on the day numbers 11–12 and from there it gradually decreases and goes below zero on day number 20 and again the temperature difference is enhanced to above 20 K on day numbers 22–25. So, from the observations, it is apparent that SSW events occurred around day numbers 3–5, 8–19 and 21–32. The Kp index and F10.7 cm flux show that except on day number 27, all these days are magnetically quiet and solar flux is low.

3.2. Day-to-Day Variability of EEJ Strength and TEC Over Bhopal

[10] In order to study the day-to-day variabilities in TEC over Bhopal which is close to EIA region and EEJ strength over Indian region and their association with each other during the major SSW events during January 2006, we present the daily variation of GPS TEC along with daily variation of EEJ strength (ΔH) obtained during January 2006. Figure 3a shows the daily temporal variation of EEJ strength over the time period 06:00–20:00 Indian Standard Time (IST) (IST = UT + 5.5) for the month of January 2006. Here it may be mentioned that longitude of 82.5°E is the longitude reference for IST. Also plotted is the mean EEJ strength averaged during 1–5 January 2006 as a reference which is shown in red color. It may be noted that all the days during January 2006 are geomagnetically quiet days. Figure 3b shows the daily temporal variation of TEC over Bhopal over the time period 06:00–20:00 IST for January 2006 in TEC units (1 TEC unit = 1.0×10^{16} ele/m^2). It may be noted here that only signal paths with elevation angles above 30° are utilized to obtain TEC from GPS observations to reduce the effects of multipath. Also superimposed in the each subplot in the figures is the 5 min mean TEC averaged for 1–5 January 2006 similar to that of EEJ strength. From both these figures, it is seen that as EEJ strength varies TEC over Bhopal also varies. The important thing to notice from the figure is that EEJ strength goes negative on 12, 14, 15 and 16 January 2006 and also on 27–30 January 2006 in the afternoon hours. It may be pointed out here that whenever ΔH goes negative with $\Delta H < -50$ nT or so, that day is

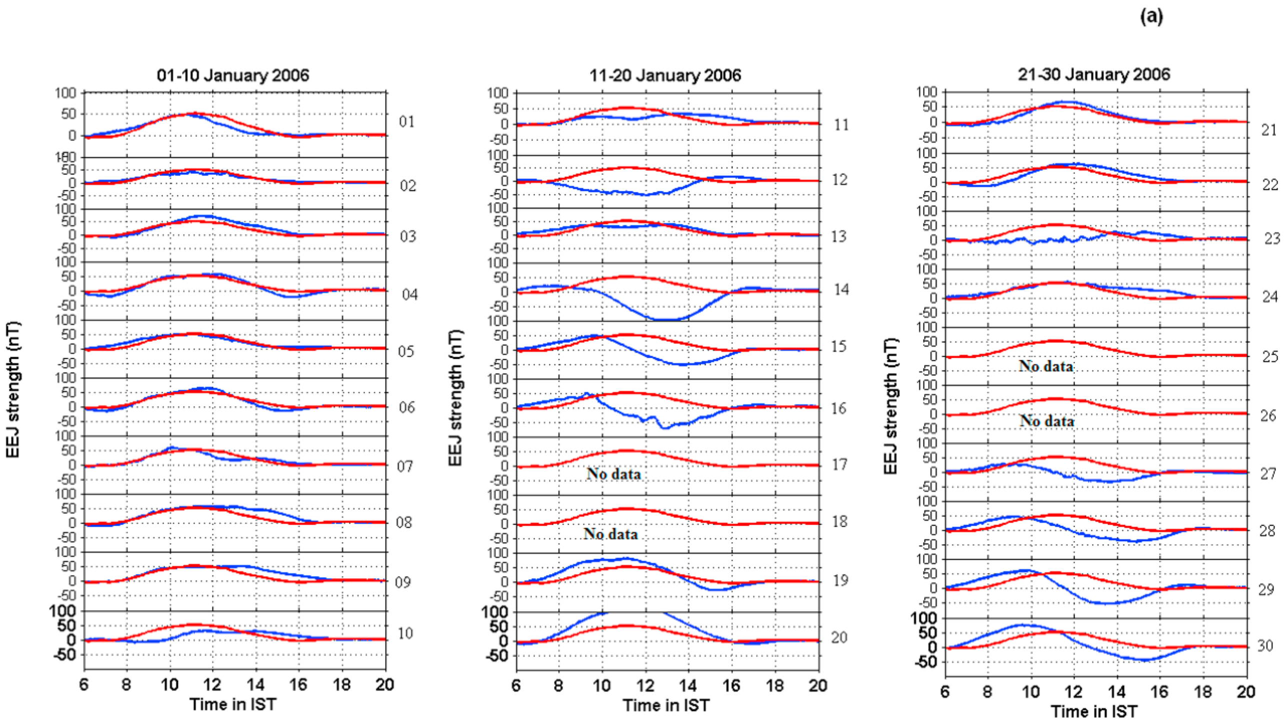

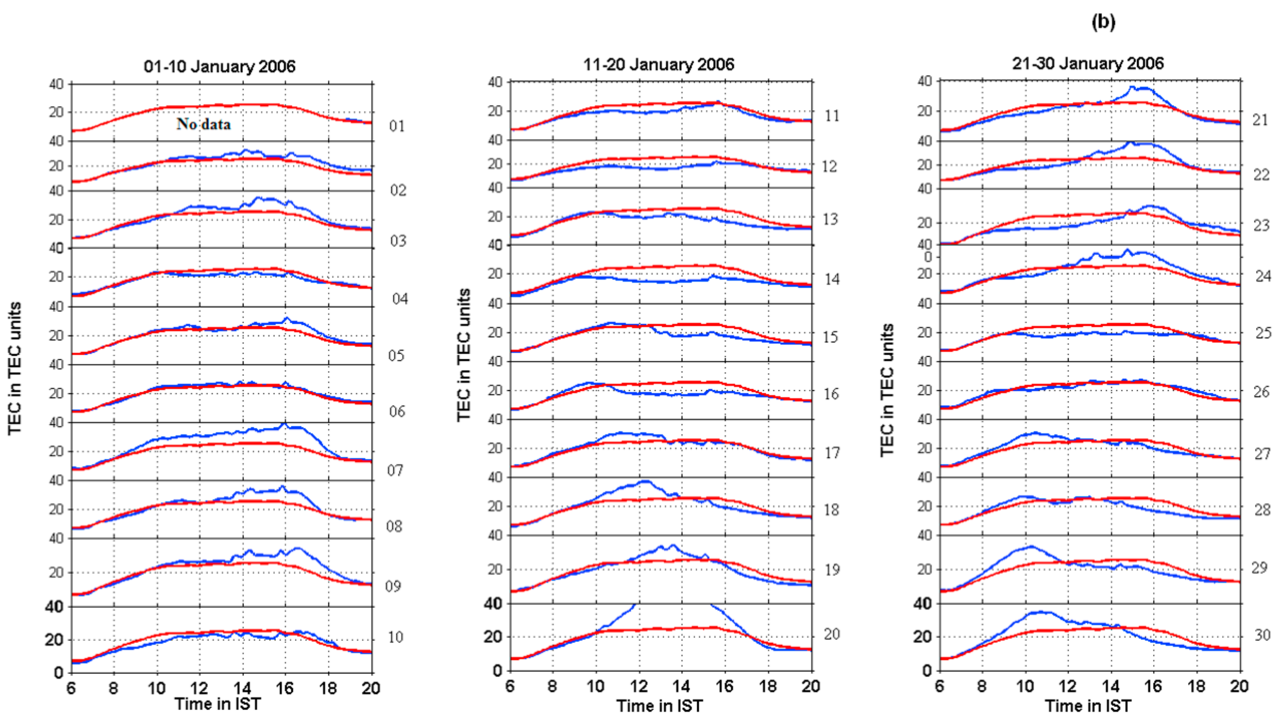

Figure 3. The daily temporal variability of (a) EEJ strength and (b) GPS TEC over Bhopal near anomaly crest region over the time period 06:00–20:00 IST during 01–30 January 2006. Also superimposed in each subplot is the mean EEJ strength and mean TEC respectively (shown in red color).

considered as a strong counter electrojet (CEJ) event. On all these days, TEC over Bhopal also shows a reduction as in the EEJ strength. Since ΔH goes negative in the afternoon hours, TEC over Bhopal shows enhancements during morning hours, during 27–30 January 2006.

3.3. Temporal and Latitudinal Variation of EEJ Strength and TEC Over India

[11] In order to see whether any correlation exists among the variabilities in GPS TEC at different latitudes and EEJ strength during these major SSW events, (a) the daily EEJ

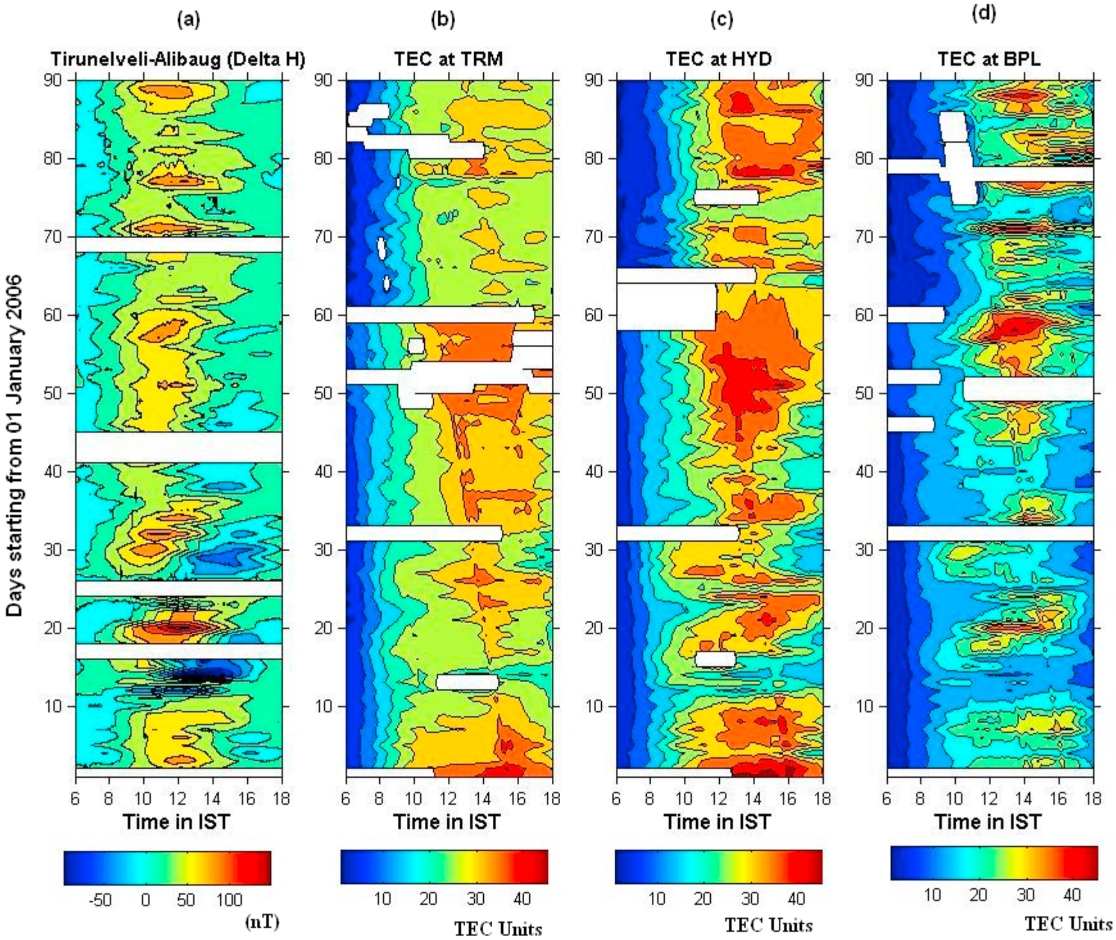

Figure 4. The contour map of (a) EEJ strength and TEC over (b) Trivandrum, (c) Hyderabad and (d) Bhopal stations respectively.

strength and TEC obtained at (b) Trivandrum, (c) Hyderabad and (d) Bhopal respectively averaged for every 5 min interval are plotted during 06:00 to 18:00 IST for January to March 2006 in Figures 4a–4d as contour maps. Here it may be noted that while horizontal axis represents the time in IST, vertical axis represents the day number. The color bar represents nT for EEJ strength and TEC units for TEC respectively. Further, it may be noted that the white gaps in the figure represents data gap either due to non-availability of the data or due to the elevation threshold used, since we have used elevation angles of >30°, in obtaining this figure. Figure 4a shows that EEJ strength is modulated in the form of highs and lows during Days 5–40. The TEC observations shown in Figures 4b–4d for the stations Trivandrum, Hyderabad and Bhopal also reveal some modulations in TEC in accordance with EEJ strength but the modulation is found to be most pronounced for Bhopal as shown in the figure.

[12] Figures 5a and 5b show the smoothed mean EEJ strength and TEC over Bhopal at (*i*) 10:00–10:30 IST, (*ii*) 14:00–14:30 IST and (*iii*) 16:00–16:30 IST respectively during January to February 2006 as shown in the subplots starting at the top. In these plots, the red star represents 5-point running averages while the blue hexagon represents 3-point running averages. This type of smoothing was resorted to in order to bring out any signature of oscillations on PW time scales (12–16 days). The figure suggests that clearly there exists this type of oscillatory behavior exists in both EEJ strength and TEC over Bhopal during the periods of SSW warming events throughout January 2006 and extending to few days in February 2006. The oscillations in EEJ show a shift of the phase to later local times as the days progress. In order to study the correlation among EEJ and TEC over Hyderabad and Bhopal respectively, we have plotted the correlation plots in Figures 6a–6d. Here while left plots show the correlation between mean EEJ strength and TEC over Hyderabad at (*i*) 14:00–14:30 IST and (*ii*) 16:00–16:30 IST respectively, right plots show the same for Bhopal station. From the figure, it is clear that EEJ strength and TEC over Hyderabad are correlated even during afternoon CEJ implying that EEJ in the morning hours lifted the plasma over the equator sufficiently high to altitudes ~400 km that the plasma could diffuse down geomagnetic field lines to F region heights over Hyderabad (see Figure 1b). However, the plasma would have to be lifted above 700 km in order for it to diffuse down to the *F* region over Bhopal. On the days with afternoon CEJ, the anomaly region may not have extended to Bhopal during the morning EEJ period. Hence the correlation between EEJ and Bhopal TEC differ from that between EEJ and

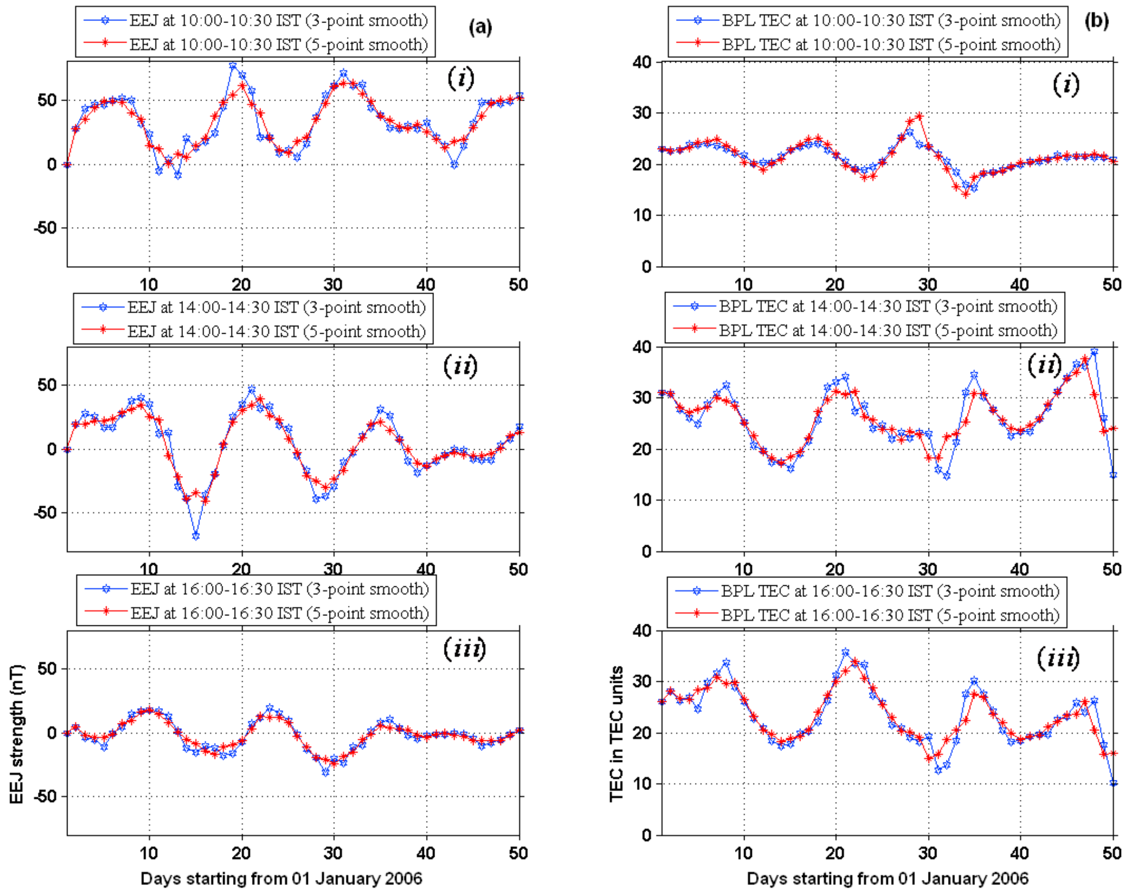

Figure 5. The daily mean (a) EEJ strength and (b) TEC over Bhopal at (*i*) 10:00–10:30 IST, (*ii*) 14:00–14:30 IST and (*iii*) 16:00–16:30 IST respectively during Jan–Feb 2006. Here, the red star represents 5-point running average while the blue hexagon represents 3-point running average.

Hyderabad TEC with afternoon TEC at Bhopal rising more rapidly with EEJ strength than the afternoon TEC at Hyderabad when no CEJ is present during the afternoon hours under consideration.

[13] Further, to study the latitudinal distribution of mean TEC over a period of 14:00–16:00 IST, the daily mean TEC as a function of latitude and day number are plotted during January to March 2006 which is obtained after combining all 18 stations of data as shown in Figure 7a. It may be noted that we have used signal path elevation angles >30°, latitude bin of 2° and longitude range of 75–85 degrees in obtaining this figure. From the figure, it can be noticed that in the first 40 days TEC has undergone major modulation in the latitudinal distribution. In order to study the variation of maximum TEC during the time period considered here and its corresponding latitude, the daily maximum TEC and its corresponding latitude are plotted as a function of day number as shown in Figures 7b and 7c. It may be noted that while the y axis represents day number, x axis represents maximum TEC in Figure 7b and its corresponding latitude in Figure 7c. Also superimposed on it is their 3-point running average. From the figure, it is clear that the maximum TEC and its corresponding latitude undergoes significant changes from one day to another and represents large scale wave like oscillation in the initial period of observations.

3.4. Spectral Analysis of the EEJ Strength and TEC Over EIA

[14] Lomb-Scargle spectral analysis are applied to daily mean TEC at Bhopal and mean EEJ strength obtained at 3 time interval viz.: 10:00–10:30 IST, 14:00–14:30 IST and 16:00 to 16:30 IST to study the wave periods. Lomb-Scargle periodogram analysis was used rather than Fast Fourier Transform (FFT) analysis because the Lomb-Scargle periodogram is equivalent to least squares fitting of sine waves and is a frequency analysis tool commonly used with unevenly spaced data [*Lomb*, 1976; *Scargle*, 1982]. Hence this technique is better able to deal with data sets with missing points. Figures 8a and 8b show the amplitude spectra of mean EEJ strength data and mean TEC over Bhopal station respectively as obtained from Lomb-Scargle method. Different color code indicates different times. The spectral analysis suggests that for data obtained during Jan–March, 2006, the dominant periods are found to be close to 13–14-days in both EEJ strength and TEC observations. Figures 9a–9d show the EEJ strength and TEC over Bhopal and their wavelet analysis using high resolution continuous data. The observations suggest that EEJ strength and TEC have diurnal and semi-diurnal amplitudes apart from quasi 2 day, 16 day wave periods. While 2-day wave is pronounced in the EEJ during day numbers 10–15, very weak 2-day wave

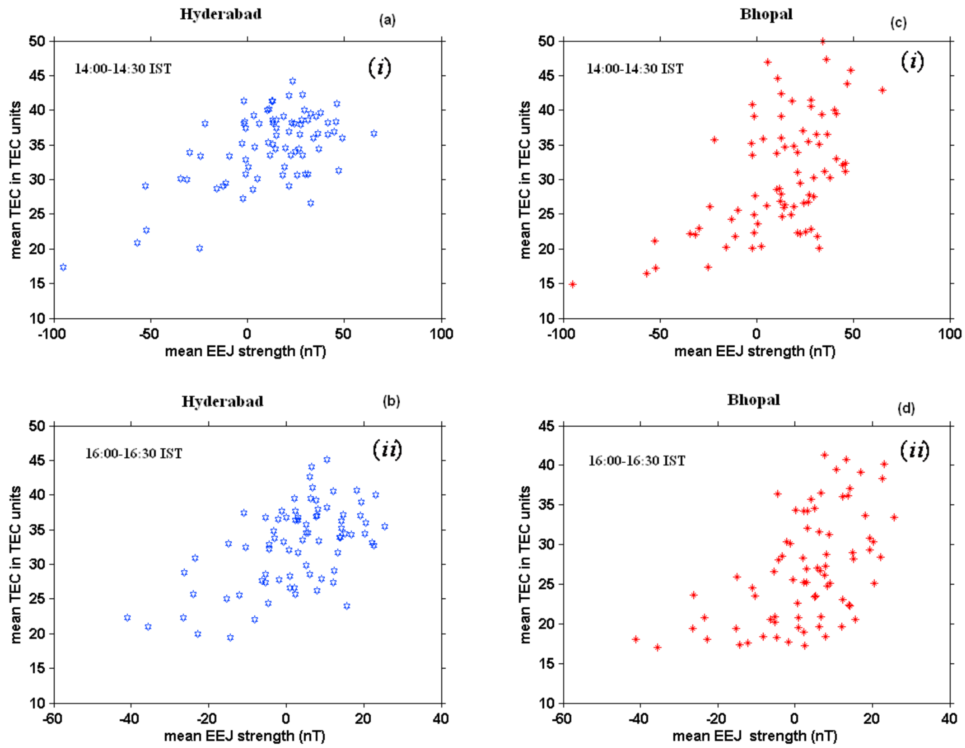

Figure 6. The correlation between average EEJ strength and TEC over (a, b) Hyderabad and (c, d) Bhopal stations at (*i*) 14:00–14:30 IST and (*ii*) 16:00–16:30 IST respectively.

is observed around day number 5 and day numbers 20–25 in TEC observations. The semi-diurnal amplitude in Bhopal TEC shows a very large value around day number 19. Figure 10 shows the cross-wavelet spectrum of EEJ strength and TEC over Bhopal during January month obtained using the method described in *Torrence and Webster* [1999]. The observations suggest that there exists a significant power at diurnal, semi-diurnal and 16 day periods. Also, the cross-wavelet spectrum indicates the existence of some power in quasi 2-day wave period at day numbers 5, 10–15 and 20–25.

4. Discussion

[15] In recent years there have been several studies on the impact of SSW events on the equatorial and low latitude ionosphere [*Sathishkumar and Sridharan*, 2009; *Sridharan et al.*, 2009; *Vineeth et al.*, 2009; *Chau et al.*, 2009; *Fejer et al.*, 2010; *Goncharenko et al.*, 2010b]. The observations presented in section-3 above suggest the following points: (a) large-scale wave like structures in the EEJ strength and GPS TEC observations during SSW events that occurred around day numbers 3–5, 8–19 and 21–32, (b) strong correlation of variabilities in the EEJ strength and latitudinal variation of maximum TEC, (c) quasi 16 day wave period in both EEJ strength and TEC observations, (d) no periodic waves observed around quasi 16-day period in solar flux at F10.7 and Kp index and (e) semi-diurnal signature in EEJ strength and TEC over EIA region. A recent study using SKiYMET radar over Trivandrum shows existence of quasi 16-day wave periods in zonal winds in the MLT region during the same period [*Das et al.*, 2010]. An investigation of the variability of mesospheric tides observed near the dip equator during major SSW events has shown an enhancement of the semi-diurnal tidal amplitude in the zonal wind at 88 km during the period 13–30 Jan, 2006 resulting in the semi-diurnal tide being larger than the diurnal tide amplitude during this period when CEJs attributed to the SSW events were also observed [*Sridharan et al.*, 2009]. CEJs related to SSWs have also been reported by *Vineeth et al.* [2009], who observed the stratospheric temperature at ~30 km over the dip equatorial region to suddenly decrease before the SSWs and related CEJs. The effect of SSW on TEC in the region near the EIA crest has been studied using global ionospheric maps [*Pedatella and Forbes*, 2010; *Goncharenko et al.*, 2010b]. In the present paper, the EEJ/CEJ phenomena in the dip equatorial ionosphere over the Indian longitude (70–90°E) region have been examined along with simultaneous GPS TEC data extending up to ~20°N geomagnetic latitude, to study the nature and magnitude of the *E* region and *F* region effects of the SSW events of 2005/2006.

[16] In the present study, quasi-16-day wave periods are seen in both EEJ strength derived from geomagnetic field observations and GPS-TEC over Bhopal (BPL), a station close to the EIA crest, in association with the SSW events of January 2006. The effects of SSW events on TEC measured at stations Trivandrum (TRM) close to the dip equator and Hyderabad (HYD), at geomagnetic latitude of about 8°N are not as pronounced as on the TEC obtained over Bhopal (BPL) (Figure 4). This latter observation is in agreement with that of *Pedatella and Forbes* [2010], who concluded that the concentration of the variations in GPS TEC associated with SSW events in the EIA crest region indicated that they are linked with the changes in the equatorial E region dynamo generated electric fields. Variation of these dynamo

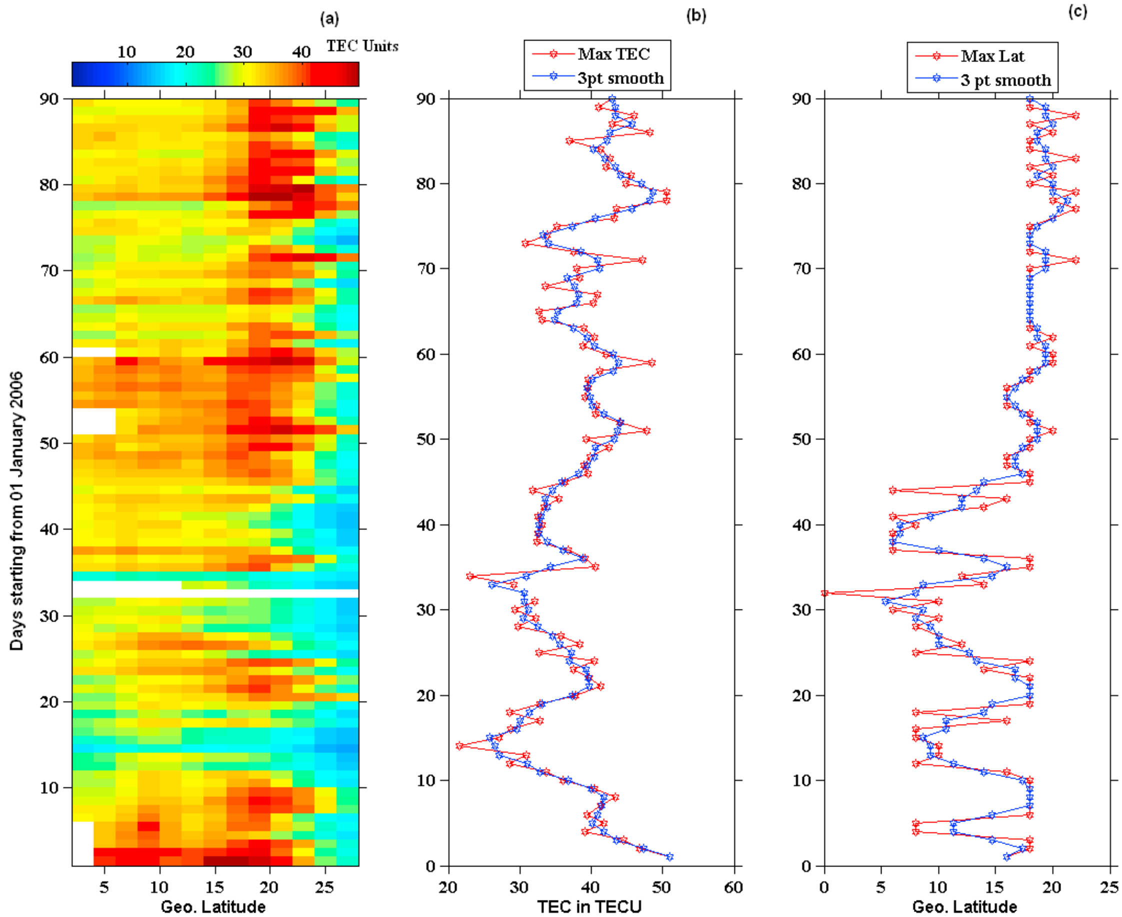

Figure 7. (a) The contour map of latitudinal distribution of mean TEC during 14:00–16:00 IST as a function of latitude and day number during January to March 2006. (b, c) The variation of maximum TEC and its corresponding latitude. Also shown is the 3-point running average.

region electric fields are reflected in the variations of the EEJ strength [*Fejer et al.*, 2010] and the equatorial E × B drift of the *F* region [*Chau et al.*, 2009]. Our results show how variations in the E region dynamo generated electric fields in response to SSW events as seen in the EEJ strength produce change in the distribution of plasma throughout the low-latitude ionosphere. As a result, apart from the strength of the EIA, the latitude of maximum TEC also shows a pronounced quasi-16-day oscillation (Figure 7) in Jan–Feb 2006, as expected from such oscillation in the equatorial E region electric field.

[17] The Lomb-Scargle (L-S) periodogram of EEJ and the TEC over BPL during three different daytime intervals, for Jan–Mar 2006 show a dominant period of about 13–14 days (Figure 8). In the TEC over BPL, there is significant oscillation with a period between 25 and 30 days. Such an oscillation may be associated with geomagnetic activity recurring with an approximately 27 day period, due to solar wind high speed streams coming from coronal holes during the declining phase of a solar cycle or with a ~27 day period in solar EUV flux. Plots of the power spectra of variations in Kp Index and solar EUV flux are not included in this paper because Lomb-Scargle periodograms of the Kp index and SOHO 0.1–50 nm EUV flux for the period 01 December 2005–01 March 2006 have been shown in the paper by *Pedatella and Forbes* [2009]. From *Pedatella and Forbes* [2009, Figure 2], it is seen that strong oscillations of ~24 day period are present in the SOHO EUV flux and a broad 28 day peak is seen in Kp. The largest peak in Kp variations has a period of 9-days, which is attributed to solar wind high-speed streams during the interval under consideration [*Thayer et al.*, 2008], and this is considerably stronger than a peak near 16 days. A 10 day peak is seen in both EEJ and TEC at BPL, which is considerably weaker than the quasi-16 day peak. In their study of the modulation of the equatorial F region by the quasi-16 day PW using CHAMP electron densities and TEC measurements from global ionospheric maps for the period 1 December 2005 to 1 March 2006, *Pedatella and Forbes* [2009] go on to conclude that the quasi-16-day oscillation in these ionospheric parameters are not due to recurrent geomagnetic activity or solar flux variability, but due to the coupling of the ionosphere with lower atmosphere. The results of the present paper show that the *F* region electron densities, which contribute the most to TEC vary significantly in response to the 27-day oscillations in EUV flux, while the EEJ strength shows a much weaker response. The largest response of both EEJ and TEC over Bhopal is to the tides modulated by the quasi-16-day PW.

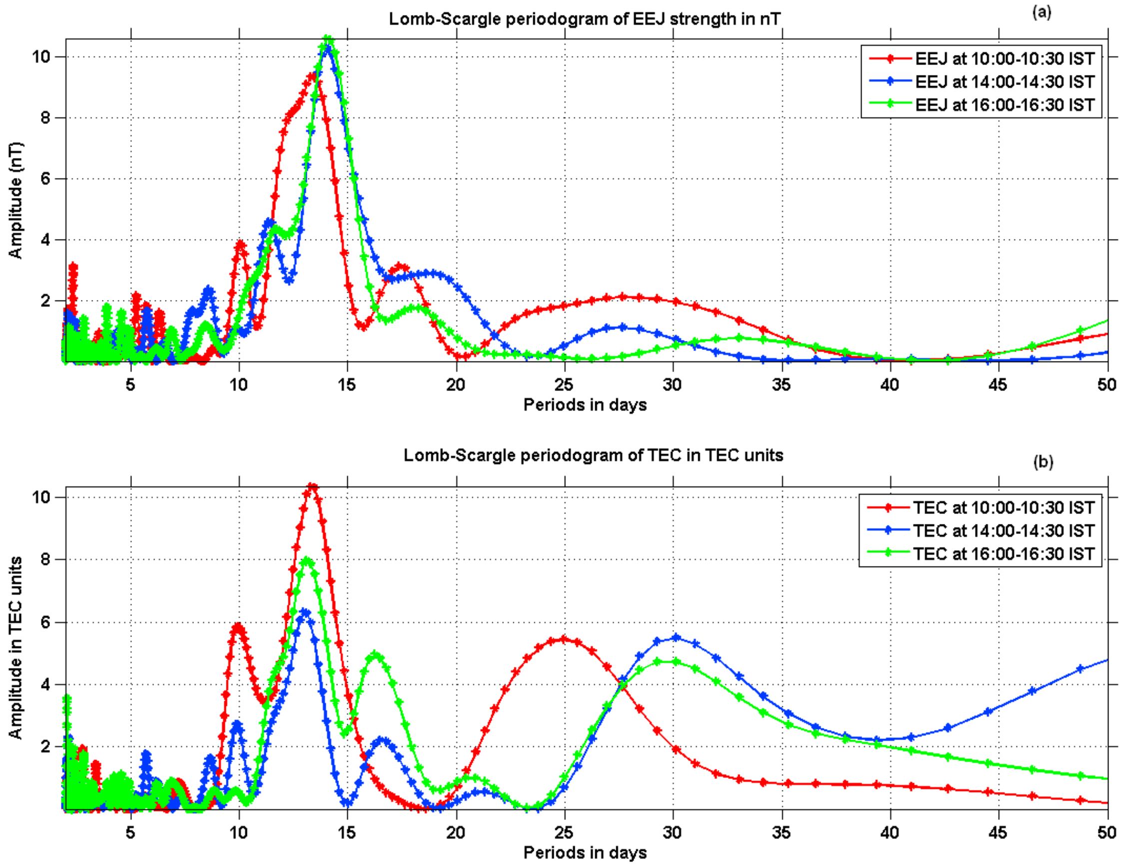

Figure 8. The Lomb-Scargle analysis of (a) mean EEJ strength and (b) mean TEC over Bhopal at 10:00–10:30 IST, 14:00–14:30 IST and 16:00–16:30 IST respectively.

[18] Morlet wavelet analysis of EEJ strength clearly shows the presence of quasi-16-day oscillations during all of January 2006. There is also an enhancement of the semi-diurnal amplitude during January 13–February 3, 2006, when the occurrence of afternoon CEJs was enhanced. For the TEC over BPL, near the crest of the EIA, wavelet spectrum also shows the presence of quasi-16-day oscillations in January 2006, although for a shorter duration than in the case of the EEJ. For GPS-TEC observations restricted to a fixed longitude range (75–90°E), it is not possible to isolate a zonally symmetric non-oscillatory contribution (identified by n = 0 and s = 0 in *Pedatella and Forbes* [2010]) to the GPS-TEC distribution. Using Global Ionospheric maps derived from GPS-TEC observations, *Pedatella and Forbes* [2010] demonstrated that this contribution to GPS-TEC is closely related to the Kp index, even during periods with little geomagnetic activity. Hence the 10 day and 25–30 day peaks seen in the L-S periodogram of TEC over BPL at 3 different time intervals may be attributed to this zonally symmetric contribution related to geomagnetic activity. Since this component has nothing to do with atmospheric tide generated *E* region electric fields, oscillations of periods ~27 days in EEJ strength are not pronounced. This is also supported by *Pedatella and Forbes* [2010, Figure 1a], which does not show any variation with magnetic latitude of the n = 0, s = 0 component of GPS-TEC. This difference in the behavior of the spectra for EEJ strength and TEC over BPL indicates that the wavelet spectra for the two would also differ. However, the cross-wavelet spectrum of EEJ strength and TEC over BPL for the interval January–March 2006 clearly shows that perturbation of the semi-diurnal tides by quasi-16-day PW arising due to SSW events modulates the *E* region dynamo electric fields which cause quasi-16-day variations in both the EEJ strength and GPS-TEC near the EIA crest. The associated change in semi-diurnal tides appear to be most prominent around January 18 and 28, 2006.

[19] *Chau et al.* [2010] studied the quiet time ionospheric variability over Arecibo, Puerto Rico during January–February 2008/2009 when SSWs are prominent using incoherent scatter radar electron density and temperature measurements and GPS TEC. Their observations show strong ionospheric perturbations in the daytime TEC near Arecibo and strong vertical drift velocity perturbations near equator occur at the same time after SSW events. As suggested by *Chau et al.* [2010], we believe that the efficiency of the planetary waves during low solar activity period increases in perturbing E region drifts, electric fields and GPS TEC at EIA due to modulation of E region dynamo. *Goncharenko et al.* [2010b] have studied the response of ionospheric TEC to several SSW events during winter months of 2008/2009 and suggested that ionospheric perturbations at low latitudes usually begin a few days after peak in the stratospheric temperature and are observed as an enhancement of EIA in the morning sector and a suppression of EIA in the afternoon hours. *Liu et al.* [2010] have

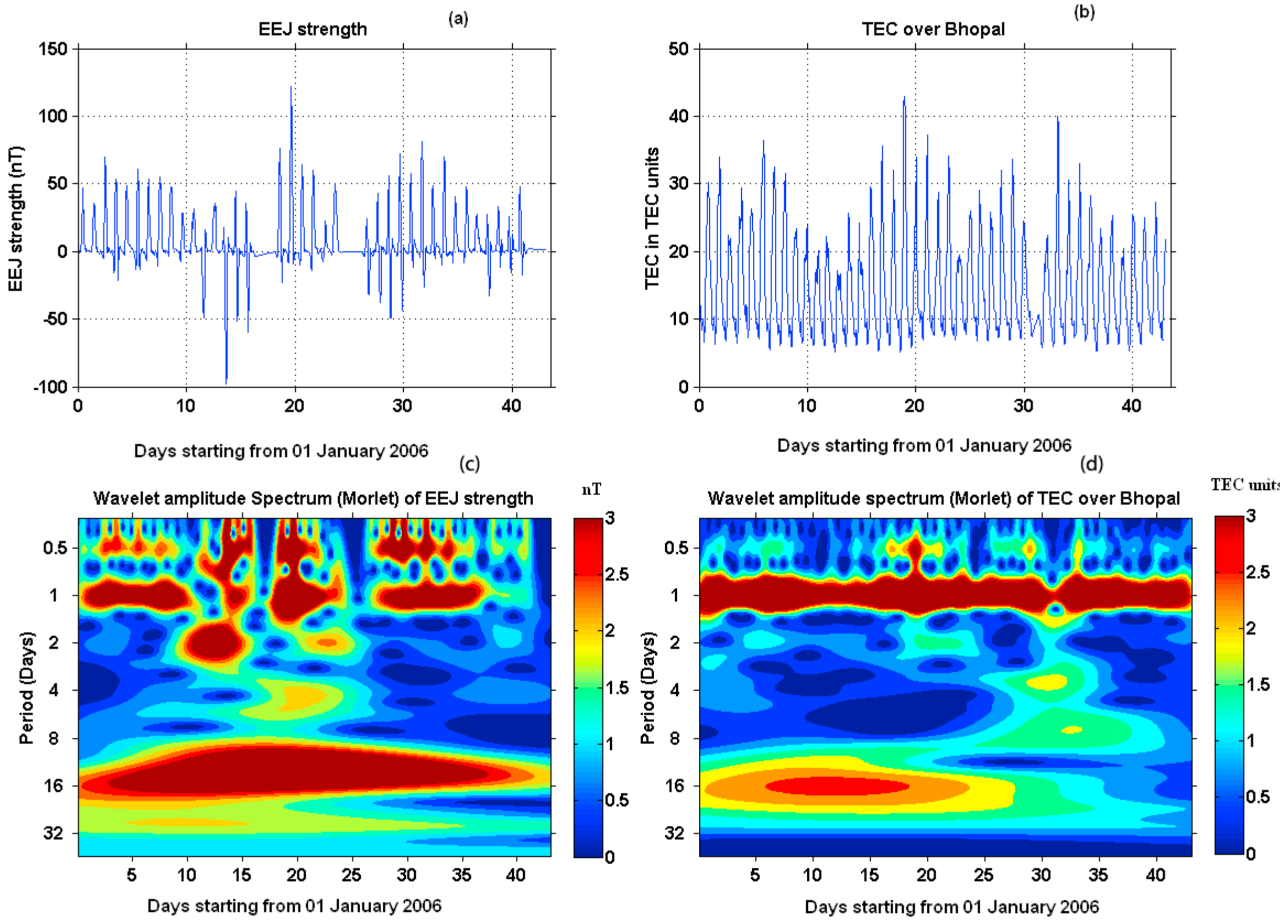

Figure 9. (a) EEJ and (b) TEC over Bhopal during January 2006 period and (c, d) their wavelet (Morlet) analysis.

also studied the ionospheric variability when planetary wave is excited in the winter stratosphere using TIME-GCM model. Their observations suggested that the ionospheric changes are dependent on both the longitude and local time and are determined by the amplitudes and phases of the interacting waves. Recent results of ionospheric electron density using COSMIC during SSW events suggest that competing roles of electric field, neutral wind and composition may cause the complex electrodynamical features that result in the variability of the ionosphere at different latitudes during SSW events [*Yue et al.*, 2010]. Using the observations presented here, we confirm that significant vertical coupling takes place due to nonlinear interaction of PWs with atmospheric tides during major SSW events that lead to the changes in the E region electric fields and drifts, which impacts the distribution of plasma in the equatorial and low latitude ionosphere over Indian region.

5. Concluding Remarks

[20] Based on simultaneous magnetometer observations from which the EEJ strength could be derived and GPS-TEC observations over the Indian region, from which the low-latitude distribution of TEC could be derived, effects of SSW events of January 2006 on the low latitude ionosphere have been studied in this paper. The following conclusions are drawn from the present analysis:

[21] 1. The EEJ strength undergoes oscillations with a period of 13–14 days during January 2006. In these oscillations, a phase shift to later local times is seen with the progression of the days.

[22] 2. There is quasiperiodic oscillation of this type in the maximum TEC in the EIA crest region as well as in the latitude of the EIA crest. The oscillations are more pronounced near the EIA crest, as compared to other latitudes.

[23] 3. The L-S periodogram of GPS-TEC over Bhopal near the EIA crest during three different time intervals shows the presence of oscillations of 13–14 days and a peak around 10 days. These latter oscillations are attributed to a zonally symmetric contribution to the GPS-TEC distribution arising from variations in geomagnetic activity as measured by the Kp index [*Pedatella and Forbes*, 2010]. Oscillations with these periods (∼10 days) are not so pronounced in the EEJ strength, where the dominant process is the modulation of the *E* region dynamo electric field by the interaction between quasi-16-day PWs and semi-diurnal tides.

[24] 4. Modulation of the *E* region dynamo electric field arising due to SSW events of January 2006 is the dominant source of quasi-16-day oscillations in the GPS-TEC near the

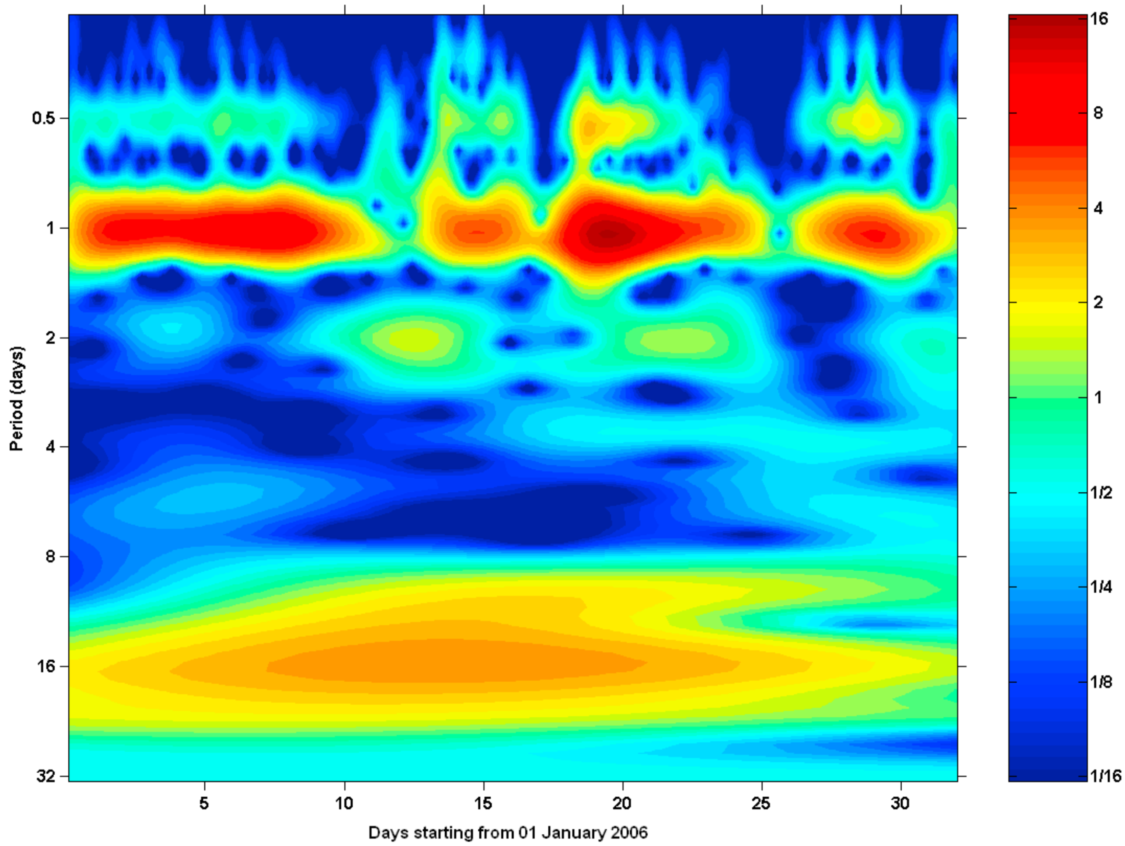

Figure 10. The cross-wavelet analysis of EEJ strength and TEC over Bhopal during January 2006.

EIA crest as seen from the cross-wavelet spectrum of EEJ strength and TEC over Bhopal for January 2006.

[25] **Acknowledgments.** The research work presented here is carried out through the financial support from CAWSES India phase-2 project of Indian Space Research Organization (ISRO), Government of India. The authors are thankful to Space Application Centre, ISRO, Ahmedabad, and their technical staff for providing the GAGAN data. The authors also would like to thank WDC geomagnetic data center, Kyoto University, for providing geomagnetic indices and NGDC for providing solar flux data. Thanks also go to Sobhana Alex of Indian Institute of Geomagnetism, Navi Mumbai, for providing processed geomagnetic data.

[26] Robert Lysak thanks the reviewers for their assistance in evaluating this paper.

References

Alex, S., and R. G. Rastogi (1989), Day-to-day variability of maximum electron density and ionospheric electron content at equatorial stations, *Indian J. Radio Space Phys.*, *18*, 99–102.

Anderson, D. N., A. Anghel, K. Yumoto, M. Ishituka, and E. Kudeki (2002), Estimating daytime, vertical E × B drift velocities in the equatorial *F* region using ground-based magnetometer observations, *Geophys. Res. Lett.*, *29*(12), 1596, doi:10.1029/2001GL014562.

Araujo-Pradere, E. A., T. J. Fuller-Rowell, M. V. Codrescu, and D. Bilitza (2005), Characteristics of the ionospheric variability as a function of season, latitude, local time, and geomagnetic activity, *Radio Sci.*, *40*, RS5009, doi:10.1029/2004RS003179.

Bagiya, M. S., H. P. Joshi, K. N. Iyer, M. Aggarwal, S. Ravindran, and B. M. Pathan (2009), TEC variations during low solar activity period (2005–2007) near the Equatorial Ionospheric Anomaly Crest region in India, *Ann. Geophys.*, *27*, 1047–1057, doi:10.5194/angeo-27-1047-2009.

Balan, N., and K. N. Iyer (1983), Equatorial anomaly in ionospheric electron content and its relation to dynamo currents, *J. Geophys. Res.*, *88*(A12), 10,259–10,262, doi:10.1029/JA088iA12p10259.

Chau, J. L., B. G. Fejer, and L. P. Goncharenko (2009), Quiet variability of equatorial E × B drifts during a sudden stratospheric warming event, *Geophys. Res. Lett.*, *36*, L05101, doi:10.1029/2008GL036785.

Chau, J. L., N. A. Aponte, E. Cabassa, M. P. Sulzer, L. P. Goncharenko, and S. A. González (2010), Quiet time ionospheric variability over Arecibo during sudden stratospheric warming events, *J. Geophys. Res.*, *115*, A00G06, doi:10.1029/2010JA015378.

Dabas, R. S., P. K. Bhuyan, T. R. Tyagi, R. K. Bhardwaj, and J. B. Lal (1984), Day-to-day changes in ionospheric electron content at low latitudes, *Radio Sci.*, *19*(3), 749–756, doi:10.1029/RS019i003p00749.

Das, S. S., K. K. Kumar, S. B. Veena, and G. Ramkumar (2010), Simultaneous observation of quasi 16 day wave in the mesospheric winds and temperature over low latitudes with the SKiYMET radar, *Radio Sci.*, *45*, RS6014, doi:10.1029/2009RS004300.

Fagundes, P. R., J. A. Bittencourt, J. R. Abalde, Y. Sahai, M. J. A. Bolzan, V. G. Pillat, and W. L. C. Lima (2009a), *F* layer postsunset height rise due to electric field prereversal enhancement: 1. Traveling planetary wave ionospheric disturbance effects, *J. Geophys. Res.*, *114*, A12321, doi:10.1029/2009JA014390.

Fagundes, P. R., J. R. Abalde, J. A. Bittencourt, Y. Sahai, R. G. Francisco, V. G. Pillat, and W. L. C. Lima (2009b), *F* layer postsunset height rise due to electric field prereversal enhancement: 2. Traveling planetary wave ionospheric disturbances and their role on the generation of equatorial spread *F*, *J. Geophys. Res.*, *114*, A12322, doi:10.1029/2009JA014482.

Fejer, B., E. de Paula, S. González, and R. Woodman (1991), Average vertical and zonal *F* region plasma drifts over Jicamarca, *J. Geophys. Res.*, *96*(A8), 13,901–13,906, doi:10.1029/91JA01171.

Fejer, B. G., M. E. Olson, J. L. Chau, C. Stolle, H. Luhr, L. P. Goncharenko, K. Yumoto, and T. Nagatsuma (2010), Lunar-dependent equatorial ionospheric electrodynamic effects during sudden stratospheric warmings, *J. Geophys. Res.*, *115*, A00G03, doi:10.1029/2010JA015273.

Forbes, J. M., and S. Leveroni (1992), Quasi 16-day oscillation in the ionosphere, *Geophys. Res. Lett.*, *19*, 981–984, doi:10.1029/92GL00399.

Forbes, J. M., S. E. Palo, and X. Zhang (2000), Variability of the ionosphere, *J. Atmos. Sol. Terr. Phys.*, *62*, 685–693, doi:10.1016/S1364-6826(00)00029-8.

Fuller-Rowell, T. J., M. V. Codrescu, B. G. Fejer, W. Borer, F. Marcos, and D. N. Anderson (1997), Dynamics of the low-latitude thermosphere: Quiet and disturbed conditions, *J. Atmos. Sol. Terr. Phys.*, *59*, 1533–1540, doi:10.1016/S1364-6826(96)00154-X.

Fuller-Rowell, T., F. Wu, R. Akmaev, T.-W. Fang, and E. Araujo-Pradere (2010), A whole atmosphere model simulation of the impact of a sudden stratospheric warming on thermosphere dynamics and electrodynamics, *J. Geophys. Res.*, *115*, A00G08, doi:10.1029/2010JA015524.

Goncharenko, L. P., J. L. Chau, H.-L. Liu, and A. J. Coster (2010a), Unexpected connections between the stratosphere and ionosphere, *Geophys. Res. Lett.*, *37*, L10101, doi:10.1029/2010GL043125.

Goncharenko, L. P., A. J. Coster, J. L. Chau, and C. E. Valladares (2010b), Impact of sudden stratospheric warmings on equatorial ionization anomaly, *J. Geophys. Res.*, *115*, A00G07, doi:10.1029/2010JA015400.

Gupta, J. K., and L. Singh (2000), Long term ionospheric electron content variations over Delhi, *Ann. Geophys.*, *18*, 1635–1644, doi:10.1007/s00585-001-1635-8.

Hoffmann, H., W. Singer, D. Keuer, W. K. Hocking, M. Kunze, and Y. Murayama (2007), Latitudinal and longitudinal variability of mesospheric winds and temperatures during stratospheric warming events, *J. Atmos. Sol. Terr. Phys.*, *69*, 2355–2366, doi:10.1016/j.jastp.2007.06.010.

Liu, H.-L., and R. G. Roble (2002), A study of a self-generated stratospheric sudden warming and its mesospheric–lower thermospheric impacts using the coupled TIME-GCM/CCM3, *J. Geophys. Res.*, *107*(D23), 4695, doi:10.1029/2001JD001533.

Liu, H.-L., and R. G. Roble (2005), Dynamical coupling of the stratosphere and mesosphere in the 2002 Southern Hemisphere major stratospheric sudden warming, *Geophys. Res. Lett.*, *32*, L13804, doi:10.1029/2005GL022939.

Liu, H.-L., W. Wang, A. D. Richmond, and R. G. Roble (2010), Ionospheric variability due to planetary waves and tides for solar minum conditions, *J. Geophys. Res.*, *115*, A00G01, doi:10.1029/2009JA015188.

Lomb, N. R. (1976), Least-squares frequency analysis of unevenly spaced data, *Astrophys. Space Sci.*, *39*, 447–462, doi:10.1007/BF00648343.

Madden, R. A. (1979), Observations of large-scale traveling Rossby waves, *Rev. Geophys.*, *17*(8), 1935–1949, doi:10.1029/RG017i008p01935.

Mendillo, M., H. Rishbeth, R. G. Roble, and J. Wroten (2002), Modelling F2-layer seasonal trends and day-to-day variability driven by coupling with the lower atmosphere, *J. Atmos. Sol. Terr. Phys.*, *64*, 1911–1931, doi:10.1016/S1364-6826(02)00193-1.

Mukhtarov, P., D. Pancheva, B. Andonov, N. J. Mitchell, E. Merzlyakov, W. Singer, W. Hocking, C. Meek, A. Manson, and Y. Murayama (2007), Large-scale thermodynamics of the stratosphere and mesosphere during the major stratospheric warming in 2003/2004, *J. Atmos. Sol. Terr. Phys.*, *69*, 2338–2354, doi:10.1016/j.jastp.2007.07.012.

Pancheva, D., N. Mitchell, R. R. Clark, J. Drobjeva, and J. Lastovicka (2002), Variability in the maximum height of the ionospheric F2-layer over Millstone Hill (September 1998–March 2000); influence from below and above, *Ann. Geophys.*, *20*, 1807–1819, doi:10.5194/angeo-20-1807-2002.

Pancheva, D., P. Mukhtarov, N. Mitchell, D. Fritts, D. Riggin, H. Takahashi, P. Batista, B. Clemesha, S. Gurubaran, and G. Ramkumar (2008), Planetary wave coupling (5–6-day waves) in the low latitude atmosphere–ionosphere system, *J. Atmos. Sol. Terr. Phys.*, *70*, 101–122, doi:10.1016/j.jastp.2007.10.003.

Parish, H., J. M. Forbes, and F. Kamalabadi (1994), Planetary wave and solar emission signatures in the equatorial electrojet, *J. Geophys. Res.*, *99*, 355–368, doi:10.1029/93JA02096.

Pedatella, N. M., and J. M. Forbes (2009), Modulation of the equatorial *F* region by the quasi-16-day planetary wave, *Geophys. Res. Lett.*, *36*, L09105, doi:10.1029/2009GL037809.

Pedatella, N. M., and J. M. Forbes (2010), Evidence for stratosphere sudden warming-ionosphere coupling due to vertically propagating tides, *Geophys. Res. Lett.*, *37*, L11104, doi:10.1029/2010GL043560.

Rama Rao, P. V. S., S. Gopi Krishna, K. Niranjan, and D. S. V. V. D. Prasad (2006), Temporal and spatial variations in TEC using simultaneous measurements from the Indian GPS network of receivers during the low solar activity period of 2004–2005, *Ann. Geophys.*, *24*, 3279–3292, doi:10.5194/angeo-24-3279-2006.

Rastogi, R. G. (1959), The diurnal development of the anomalous equatorial belt in the F2 region of the ionosphere, *J. Geophys. Res.*, *64*(7), 727–732, doi:10.1029/JZ064i007p00727.

Rastogi, R., and J. Klobuchar (1990), Ionospheric electron content within the equatorial F2 layer anomaly belt, *J. Geophys. Res.*, *95*, 19,045–19,052, doi:10.1029/JA095iA11p19045.

Rastogi, R. G., and R. P. Sharma (1971), Ionospheric electron content at Ahmedabad (near the crest of equatorial anomaly) by using beacon satellite transmissions during half a solar cycle, *Planet. Space Sci.*, *19*, 1505–1517, doi:10.1016/0032-0633(71)90010-9.

Rastogi, R. G., R. P. Sharma, and V. Shodhan (1973), Total electron content of the equatorial ionosphere, *Planet. Space Sci.*, *21*, 713–720, doi:10.1016/0032-0633(73)90090-1.

Rishbeth, H., and M. Mendillo (2001), Patterns of F2-layer variability, *J. Atmos. Sol. Terr. Phys.*, *63*, 1661–1680, doi:10.1016/S1364-6826(01)00036-0.

Salby, M. L. (1984), Survey of planetary-scale traveling waves: The state of theory and observations, *Rev. Geophys.*, *22*(2), 209–236, doi:10.1029/RG022i002p00209.

Sathishkumar, S., and S. Sridharan (2009), Planetary and gravity waves in the mesosphere and lower thermosphere region over Tirunelveli (8.7°N, 77.8°E) during stratospheric warming events, *Geophys. Res. Lett.*, *36*, L07806, doi:10.1029/2008GL037081.

Scargle, J. D. (1982), Studies in astronomical time series analysis. II—Statistical aspects of spectral analysis of unevenly spaced data, *Astrophys. J.*, *263*, 835–853, doi:10.1086/160554.

Sethia, G., R. G. Rastogi, M. R. Deshpande, and H. Chandra (1980), Equatorial electrojet control of the low latitude ionosphere, *J. Geomagn. Geoelectr.*, *32*, 207–216, doi:10.5636/jgg.32.207.

Shepherd, M. G., D. L. Wu, I. N. Fedulina, S. Gurubaran, J. M. Russell, M. G. Mlynczak, and G. G. Shepherd (2007), Stratospheric warming effects on the tropical mesospheric temperature field, *J. Atmos. Sol. Terr. Phys.*, *69*, 2309–2337, doi:10.1016/j.jastp.2007.04.009.

Sridharan, S., S. Sathishkumar, and S. Gurubaran (2009), Variabilities of mesospheric tides and equatorial electrojet strength during major stratospheric warming events, *Ann. Geophys.*, *27*, 4125–4130, doi:10.5194/angeo-27-4125-2009.

Sripathi, S., B. Kakad, and A. Bhattacharyya (2011), Study of equinoctial asymmetry in the Equatorial Spread F (ESF) irregularities over Indian region using multi-instrument observations in the descending phase of solar cycle-23, *J. Geophys. Res.*, *116*, A11302, doi:10.1029/2011JA016625.

Thayer, J. P., J. Lei, J. M. Forbes, E. K. Sutton, and R. S. Nerem (2008), Thermospheric density oscillations due to periodic solar wind high speed streams, *J. Geophys. Res.*, *113*, A06307, doi:10.1029/2008JA013190.

Torrence, C., and P. J. Webster (1999), Interdecadal changes in the ENSO–monsoon system, *Bull. Am. Meteorol. Soc.*, *12*, 2679–2690.

Vineeth, C., T. K. Pant, C. V. Devasia, and R. Sridharan (2007), Atmosphere–ionosphere coupling observed over the dip equatorial MLTI region through the quasi 16-day wave, *Geophys. Res. Lett.*, *34*, L12102, doi:10.1029/2007GL030010.

Vineeth, C., T. K. Pant, and R. Sridharan (2009), Equatorial counter electrojets and polar stratospheric sudden warmings: A classical example of high latitude-low latitude coupling?, *Ann. Geophys.*, *27*, 3147–3153, doi:10.5194/angeo-27-3147-2009.

Yue, X., W. S. Schreiner, J. Lei, C. Rocken, D. C. Hunt, Y.-H. Kuo, and W. Wan (2010), Global ionospheric response observed by COSMIC satellites during the January 2009 stratospheric sudden warming event, *J. Geophys. Res.*, *115*, A00G09, doi:10.1029/2010JA015466.